ELSEVIER

Journal of Chromatography A, 668 (1994) 153–164

JOURNAL OF CHROMATOGRAPHY A

Studies of the interaction of NADH oxidase from *Thermus thermophilus* HB8 with triazine dyes

J. Kirchberger[a], H. Erdmann[b], H.-J. Hecht[b], G. Kopperschläger*[,a]

[a]*Institute of Biochemistry, University of Leipzig, Liebigstrasse 16, D-04103 Leipzig, Germany*

[b]*Gesellschaft für Biotechnologische Forschung mbH (GBF), Marscheroder Weg 1, D-38124 Braunschweig, Germany*

Abstract

NADH oxidase from *Thermus thermophilus* HB8 was selected to study the interaction of flavoproteins with structurally defined dye ligands. The fact that the enzyme binds NADH in addition to FAD favours the enzyme as a model for studying the interaction of enzymes with biomimetic ligands. In addition, the crystal structure of the holoenzyme is known. Applying affinity partitioning in aqueous two-phase systems, difference spectroscopy, affinity chromatography and kinetics, results about the chemistry of binding and the binding site(s) for various triazine dyes were obtained. The binding of the dyes to the enzyme is stabilized by hydrophobic and electrostatic forces. The binding behaviour is influenced by small differences in the structure of the dye ligands. In most instances the dye ligands occupy both FAD binding sites of the enzyme dimer; this is particularly shown for Procion Red H-8BN by kinetic and difference spectroscopic studies. An "optimum" structural model of a biomimetic ligand of NADH oxidase from *Thermus thermophilus* HB8 is proposed, requiring the presence of a disulphonated aminonaphthol ring combined with another aromatic negatively charged residue and a hydrophobic arm at a distance between 7 and 13 Å.

1. Introduction

The enzyme NADH oxidase from *Thermus thermophilus* HB8 catalyses the oxidation of NADH or NADPH with the formation of hydrogen peroxide in the presence of FAD, FMN or riboflavin as cofactor using oxygen as electron acceptor. In the absence of oxygen also other electron acceptors such as methylene blue, cytochrome *c* and 2,6-dichlorophenol are accepted [1]. The enzyme was found to be a dimeric flavoprotein with an apparent molecular mass of 43 600. Two molecules of FAD are bound per enzyme dimer [2].

For affinity chromatographic purification of the NADH oxidase from *Thermus thermophilus* HB8, Cibacron Blue F3G-A (CB F3G-A), a very common biomimetic dye ligand, has been used [1].

Although some data on the interaction between flavoproteins and dye ligands have already been published [3–5], the chemistry of binding and the binding site(s) are still unknown. For NADH- and ATP-dependent enzymes it has been reported that biomimetic dye ligands bind competitively to the nucleotide binding site [6]. As NADH oxidase from *Thermus thermophilus* HB8 binds NADH in addition to FAD, the latter, in contrast to many other flavoproteins, is not tightly bound, and this enzyme seems to be

* Corresponding author.

0021-9673/94/$07.00
SSDI 0021-9673(93)E1245-U

of particular interest for studying its interaction with biomimetic dye ligands. Further, a crystallographic analysis of the enzyme–dye complex appears to be feasible after the completion of the crystal structure analysis of the holoenzyme [7].

In this work, we applied the technique of affinity partitioning to study the interaction of a number of chemically defined reactive dyes with NADH oxidase. From the results of this screening procedure a set of dyes were selected to analyse the dye–enzyme interaction in more detail by application of difference spectroscopy, affinity chromatography and kinetic studies.

2. Experimental

2.1. Materials

Procion dyes were obtained from ICI Organics Division (Blackley, UK) and Cibacron dyes from Ciba Geigy (Basle, Switzerland). The dyes were deactivated and purified according to Lowe and Pearson [8] before use in difference spectroscopy and kinetics. The commercial names of the dyes are abbreviated as follows: P = Procion; C = Cibacron; B = blue; G = green; N = navy; O = orange; R = red; Y = yellow. NADH and FAD were purchased from Boehringer (Mannheim, Germany). Polyethylene glycol 6000 (PEG 6000), dextran 60 ($M_r \approx 75\,000$) and dextran 500 ($M_r \approx 450\,000$) were obtained from Serva (Heidelberg, Germany) and dextran T10 ($M_r \approx 9900$) from Pharmacia (Uppsala, Sweden). All other biochemicals were of analytical-reagent grade.

2.2. Preparation of the immobilised dye-derivatives

Dye–PEG

Triazine dyes were covalently coupled to PEG 6000 in aqueous alkaline solution and dye–PEG derivatives were purified by extraction with chloroform and followed by ion-exchange chromatography on DEAE-cellulose according to Johansson [9]. The purity of the conjugates was analysed by thin-layer chromatography on silica gel G 60 plates (Merck, Darmstadt, Germany) in 1-butanol–2-propanol–ethyl acetate–water (20:35:10:35, v/v). The cleavage of the azo linkages yielding H-E3B(M)–PEG and H-3B(M)–PEG, respectively was performed as described previously [10].

Dye–Sepharose

Procion and Cibacron dyes were coupled to Sepharose 4B as described by Hughes *et al.* [11].

2.3. Enzyme purification

NADH oxidase from *Thermus thermophilus* HB8 cloned and expressed in *Escherichia coli* has been purified by heat treatment, affinity chromatography on Blue-Sepharose and cation-exchange chromatography on S-Sepharose to homogeneity in the flavin-free form [12]. All experiments were performed with the flavin-free apoenzyme.

2.4. Enzyme assay

NADH oxidase was assayed by measuring the initial rate of oxidation of NADH at 340 nm in the presence of oxygen and FAD as described by Park *et al.* [1]. One unit of activity is defined as the amount of enzyme that converts 1 μmol of substrate per minute in 50 m*M* potassium phosphate buffer (pH 7.2) at 37°C. The protein concentration of the purified enzyme was determined spectrophotometrically at 280 nm based on $A^{1\%}_{1\,cm} = 14.88$.

2.5. Kinetics

The kinetic parameters and the inhibition constants were determined in 50 m*M* potassium phosphate buffer (pH 7.2) at 25°C by measuring the rate of oxidation of NADH at 340 nm. While varying the concentration of NADH the concentration of FAD was kept constant at 127 μM and while varying the concentration of FAD the concentration of NADH was fixed at 173 μM. The concentration of PR H-8BN–PEG was varied between 0 and 0.25 μM. The type of inhibi-

tion and the inhibition constants were calculated by non-linear regression analysis [13].

2.6. Aqueous two-phase partitioning

Two-phase systems were prepared from stock standard solutions of PEG 6000 (20%, w/w), dextran (30%, w/w) and 0.5 *M* potassium phosphate buffer (pH 7.2). The polymer concentrations are given as a percentage of the mass of the system. The amount of dye-liganded PEG given in per cent is refered to the total mass of PEG present in the system. The systems (2 g) containing about 5 units of NADH oxidase, equivalent to 58 μg of protein, were adjusted to 25°C and equilibrated by gently mixing for 30 s. After centrifugation at 1500 *g* for 5 min, samples were withdrawn from both phases for enzyme assay. Inhibition of the enzyme in the assay mixture by the dye–PEG was avoided by sufficient dilution of the samples with buffer. The partition coefficient, *K*, is defined as the ratio of the enzyme activity per unit volume in the top and bottom phases.

2.7. Affinity chromatography

Disposable columns (40 × 8 mm I.D.) (Bio-Rad Labs., Munich, Germany) containing a 1.0-ml bed volume of dye-liganded Sepharose 4B were equilibrated with 50 m*M* potassium phosphate buffer (pH 7.2) at 25°C. The dialysed enzyme was applied in excess to the column (*ca.* 35 units) and the unbound enzyme, *ca.* 2–5 units, was washed out with equilibration buffer at a flow-rate of 20 ml/h. The bound enzyme activity was eluted with equilibration buffer containing effectors as indicated in Table 6.

2.8. Difference spectroscopy

Difference spectroscopy was performed with a Specord M40 double-beam spectrophotometer (Carl Zeiss, Jena, Germany) using 50 m*M* potassium phosphate buffer (pH 7.2) at 25°C. The light path of the cuvettes was 10 mm and the spectra were recorded at a scan rate of 2 nm/s and a constant slit width of 0.5 nm. The difference spectra were recorded after adding the same amount of the dye to the reference and the sample cells, respectively, containing concentrations of the effectors and the enzyme as given in the legends of Fig. 4 and Table 3. The dye concentrations were determined spectrophotometrically by using the following molar absorption coefficients (l/mol · cm): Procion Red H-E3B (530 nm), 30 000; Procion Red H-8BN (546 nm), 21 300; Procion Red H-3B (530 nm), 18 100; Procion Red MX-8B (530 nm), 19 210; Procion Red MX-5B (523 nm), 23 690; Procion Green H-E4BD (628 nm), 45 610; Cibacron Blue F3G-A (610 nm), 13 600; and Cibacron Blue 3G-A (622 nm), 11 600.

3. Results

In order to optimize the conditions of the affinity partitioning, the distribution of the enzyme was studied in a first set of experiments as a function of the polymer concentration at a constant ratio of PEG and dextran and the relative molecular mass (M_r) of dextran (see Table 1). Systems of PEG–dextran T10 at ratios below 8:12 and systems of PEG–dextran 60 at ratios below 5:7.5 were completely miscible at 25°C. With increasing concentration of the two

Table 1
Partitioning of NADH oxidase depending on the polymer concentration and the relative molecular mass (M_r) of dextran

PEG 6000/dextran concentration ratio (w/w)	Log K^a		
	Dextran T10	Dextran 60	Dextran 500
4:6	c.m.	c.m.	−0.01
5:7.5	c.m.	−0.05	−0.12
6:9	c.m.	−0.16	−0.18
7:10.5	c.m.	−0.41	−0.20
8:12	−0.49	−0.49	−0.25
9:13.5	−0.70	−0.58	−0.29

The systems (2 g) contained 50 m*M* potassium phosphate buffer (pH 7.2), PEG 6000 (4–9%, w/w) and 5 units of purified apoenzyme. The systems were equilibrated at 25°C. The M_r values of dextrans are given under Experimental.
[a] c.m. = Complete miscibility.

polymers and by reducing the M_r of dextran, the partition coefficient of the enzyme decreased. In a system composed of 13.5% dextran T10, 9% PEG and 50 m*M* potassium phosphate buffer (pH 7.2), the partition coefficient of the enzyme was sufficiently low for the detection of changes in the partition behaviour of the enzyme caused by addition of the dye-liganded PEG to the system.

A series of 28 structurally different dyes, covalently coupled to PEG, were screened by determining the extent of the affinity partition effect (Δ log K). Δ log K was calculated from the difference in the logarithms of the partition coefficient of the enzyme in the presence and absence of the affinity ligand. In all instances 0.5% of the total PEG was replaced with dye-liganded polymer. Higher concentrations of dye–PEG led to increasing inhibition of the enzyme.

As shown in Fig. 1, the affinity partition effect of the dye ligands was heterogeneous. A number of dye ligands showed relatively low Δ log K values (PO MX-G, PO MX-2R, PY P-5GN, PY MX-R and CB BR-P), whereas others such as PN MX-RB, CR 3BA, PR H-8BN, PR H-E3B and PG H-E4BD generated a Δ log K higher than 1.5. Most of the screened dye ligands exhibited moderate Δ log K values between 0.5 and 1.5.

The strength of interaction was characterized by studying the affinity partitioning of the enzyme as a function of the concentration of selected dye ligands. With increasing concentration of dye–PEG, saturation curves were obtained as shown, for example, for CB F3G-A, PR H-8BN and PG H-E4BD in Fig. 2.

To determine the maximum extraction power (Δ log K_{max}) and the relative affinity (aff_R), defined as the ligand concentration that gener-

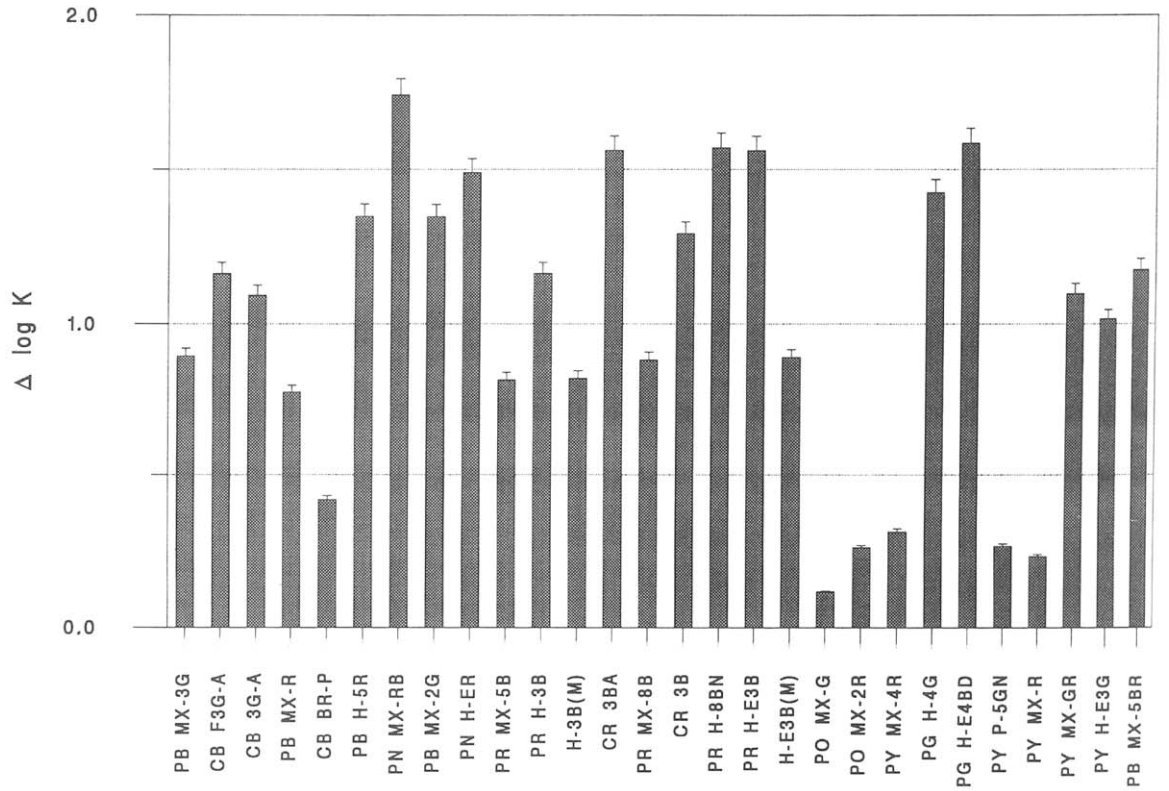

Fig. 1. Effect of diverse dye–PEG derivatives on the affinity partitioning of NADH oxidase. The systems (2 g) were composed of 13.5% (w/w) dextran T10 and 9% (w/w) PEG 6000 including 0.5% of the respective dye–PEG derivative, 50 m*M* potassium phosphate buffer (pH 7.2) and 5 units of enzyme. The systems were equilibrated at 25°C.

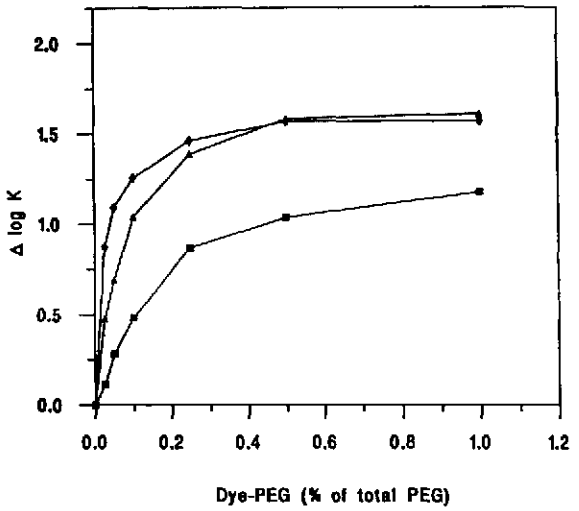

Fig. 2. Affinity partitioning of NADH oxidase as a function of the concentration of (■) CB F3G-A, (◆) PR H-8BN and (▲) PG H-E4BD covalently coupled to PEG 6000. The systems (2 g) contained 13.5% (w/w) dextran T10, 9% (w/w) PEG 6000, 50 m*M* potassium phosphate buffer (pH 7.2) and 5 units of enzyme. The partitioning was performed at 25°C.

ates 50% of Δ log K_{max}, a linear regression analysis of the double reciprocal plot was used. The highest Δ log K_{max} values were calculated for CB 3G-A, CB BR-P and PG H-E4BD (Table 2).

According to the mathematical approach of Flanagan and Barondes [14], which assumes different affinities of the dye ligand in the top and bottom phases, the dissociation constants (K_d) in both phases and the number of independent binding sites (n) were calculated by using a non-linear regression analysis [13]. The best curve fit for all dye ligands was achieved assuming two binding sites per enzyme dimer. The dissociation constants in the top phase (K_{d_T}) coincides with the values of the relative affinity (aff_R). The dissociation constant in the bottom phase (K_{d_B}) was found to be significantly lower than K_{d_T} for all dye ligands studied. Dye ligands exhibiting high affinity were PB MX-2G, PR H-E3B, PR H-8BN, PG H-E4BD and PR H-3B (azo dyes) and dyes with low affinity were CB B-RP, CB 3G-A, PB MX-3G (anthraquinone dyes) and PR MX-5B (azo dye).

By comparing the relationship between the structure of the ligand and the binding behaviour, it became obvious that small differences in the structure can cause drastic changes in the affinity to NADH oxidase. For example, a comparison of the affinities of PR H-8BN and PR MX-8B (Table 2) and the structures of these dyes (Fig. 3D) indicates that the removal of the methylanilino group gives rise to a significant decrease in the affinity of the ligand. Similar correlations were obtained after splitting off the sulphonated terminal ring(s) in PR H-E3B and PR H-3B by reducing the azo bridge with $Na_2S_2O_4$, yielding H-E3B(M) and H-3B(M), respectively, or by changing the position of the sulphonic acid group on the terminal aromatic ring from *meta/para-* (CB F3G-A) to *ortho-* (CB 3G-A) (for structures see Fig. 3C).

In order to correlate the strength of interaction with the structure of the dye ligand, difference spectroscopy was applied to the following pairs of free dyes; (A) PR H-E3B–PG H-E4BD; (B) PR H-3B–PR MX-5B; (C) CB F3G-A–CB 3G-A; and (D) PR H-8BN–PR MX-8B. The structures of these dyes are shown in Fig. 3. The results are summarized in Tables 3 and 4.

The kind of interaction was established according to Subramaniam [15] by comparing the shapes of the difference spectra of the dye–enzyme complex with that of the free dye in 0.5 *M* NaCl and 50% ethylene glycol, as shown for PR H-8BN in Fig. 4. In all instances a mixed type of hydrophobic and electrostatic interactions was found. All spectra showed one or two isosbestic points, indicating that only one class of binding sites is titrated.

Applying a non-linear regression analysis according to Barden *et al.* [16], the dissociation constants (K_d), the number of binding sites (n) and the absorption coefficients of the dye–enzyme complexes were calculated. A comparison of the dissociation constants obtained from affinity partitioning (Table 2) and difference spectroscopy is given in Table 4. The data from difference spectroscopy corroborate the existence of two binding sites for the dye per enzyme dimer. All dissociation constants are in the range of the K_m values for NADH and FAD. By

Table 2
Affinity partitioning of NADH oxidase

Dye–PEG	Double reciprocal plot (1/Δ log K *versus* 1/[Dye–PEG])		Constants calculated according to the model of Flanagan and Barondes [14]		
	Δ log K_{max}	aff_R (μM)	K_{d_T} (μM)	K_{d_B} (μM)	n
Cibacron Blue F3G-A	1.42	34.90	27.70	2.95	2
Procion Blue MX-R	1.24	26.81	23.32	2.00	2
Cibacron Blue 3G-A	2.09	91.28	55.72	19.58	2
Procion Blue B-RP	1.77	113.57	81.71	16.56	2
Procion Blue MX-3G	1.35	56.22	47.60	4.89	2
Procion Red H-E3B	1.51	4.55	3.17	0.38	2
H-E3B(M)[a]	1.02	30.29	29.50	2.02	2
Procion Blue MX-2G	1.52	3.28	2.33	0.29	2
Procion Green H-E4BD	1.77	8.61	5.45	0.84	2
Procion Red H-3B	1.43	10.47	8.14	0.85	2
H3B(M)[b]	1.60	58.10	43.99	6.58	2
Procion Red MX-5B	1.26	57.58	50.34	4.48	2
Cibacron Red 3BA	1.62	14.86	10.28	1.29	2
Procion Red MX-8B	1.24	39.76	34.79	3.00	2
Procion Red H-8BN	1.60	4.94	3.29	0.44	2
Procion Blue H-5R	1.50	15.88	11.77	1.43	2

The systems (2 g) containing 9% (w/w) PEG 6000 (0–1% dye-liganded PEG), 13.5% (w/w) dextran T10, 50 mM potassium phosphate buffer (pH 7.2) and 5 units of enzyme were equilibrated at 25°C.
[a] Procion Red H-E3B reduced with $Na_2S_2O_4$.
[b] Procion Red H-3B reduced with $Na_2S_2O_4$.

comparing the ratio of the k_{d_T}, K_{d_B} and K_d values within the four pairs of structurally related dyes a good correlation was found with both methods, with the exception of PR MX-8B–PR H-8BN.

In order to obtain information about the specificity of interactions, the influence of NADH and FAD on the affinity partitioning, the quenching effect in difference spectroscopy and the elution behaviour of the enzyme from affinity columns were studied. The affinity partitioning of the enzyme in the presence of 4 mM NADH and 2 mM FAD is shown in Table 5. To normalize the conditions of the competitive experiments, dye–PEG concentrations that were equivalent to $2K_{d_T}$ were applied. The partition coefficients of NADH and FAD were 0.88 and 1.11, respectively.

The addition of NADH caused a moderate decrease in the affinity partitioning effect (Δ log K) for all dyes studied. Only with PR MX5B a decrease in Δ log K of more than 40% was observed. The effect of FAD is more pronounced for these selected dyes. No influence could be detected with PR HE-3B and PR MX-5B. A stronger competition of the formation of the dye–enzyme complex by FAD was found with PG H-E4BD, PR MX-8B and PR H-8BN.

The influence of NADH and FAD on difference spectroscopy and on affinity chromatography is summarized in Table 6. NADH showed almost no quenching effect, with the exception of PR MX-5B. In affinity chromatography substantial amounts of enzyme were eluted with NADH when immobilized PR H-8BN, CB F3G-A and PR MX-5B were used. The stronger interfering effect of FAD was demonstrated by both methods. Minute quenching and no ability to elute the enzyme were found for PR H-E3B and PR MX-5B. However, the competition of

A

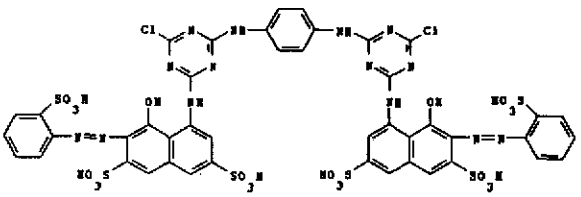

Procion Red H-E3B

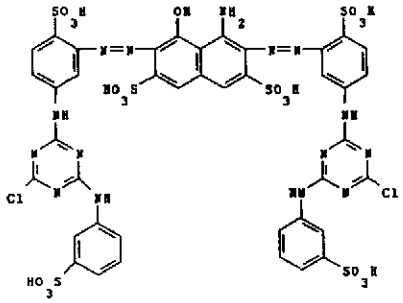

Procion Green H-4EBD

B

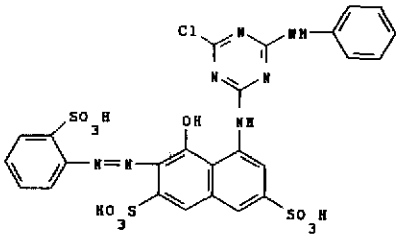

Procion Red H-3B

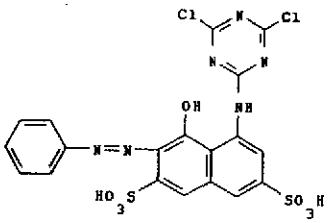

Procion Red MX-5B

C

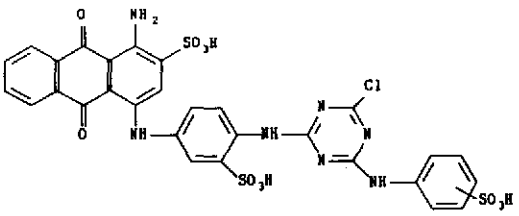

Cibacron Blue F3G-A

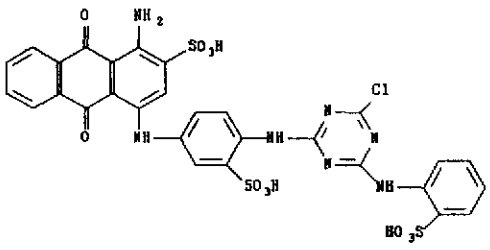

Cibacron Blue 3G-A

D

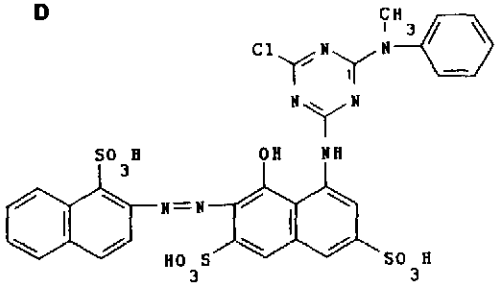

Procion Red H-8BN

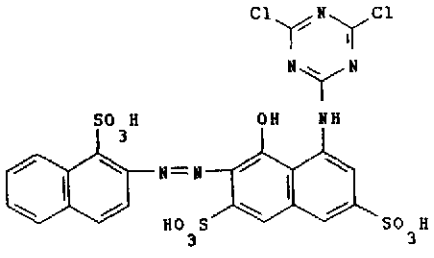

Procion Red MX-8B

Fig. 3. Structures of triazine dyes.

Table 3
Difference spectroscopy of NADH oxidase

Dye	Kind of interaction	λ_{max} (nm)	λ_{min} (nm)	Isosbestic point (nm)
Procion Red H-E3B	Mixed	555	496	510
Procion Green H-E4BD	Mixed	688	595	652
Procion Red H-3B	n.d.[a]	560	496	510
Procion Red MX-5B	Mixed	568	502	550
Procion Red MX-8B	Mixed	574	502	555
Procion Red H-8BN	Mixed	576	510	556
Cibacron Blue F3G-A	Mixed	688	586	645 and 512
Cibacron Blue 3G-A	Mixed	686	583	650 and 503

Both the sample and the reference cuvette contained 50 m*M* potassium phosphate buffer (pH 7.2). The initial enzyme concentration in the sample cuvette was 0.8–1.0 μM. The dye was added from a stock standard solution (1 m*M*) in small portions (1–5 μl) to both cuvettes. All measurements were made at 25°C.
[a] Not detectable.

FAD with the formation of the dye–enzyme complex is more pronounced with PR H-8BN, CB F3G-A, PR MX-8B and PG H-E4BD, as seen by the quenching effect and the elution recovery. The high recovery in the elution of the enzyme when using 50% ethylene glycol in buffer confirms the contribution of hydrophobic forces to the stabilization of the dye–enzyme complexes. The low recovery in the elution of the enzyme from dye-affinity columns containing PR H-8BN and CB F3G-A as immobilized ligands (Table 6) can be increased significantly without decreasing of the purification factor by addition of 25% (v/v) ethylene glycol to the NADH-containing elution buffer.

The kinetic analysis of the NADH oxidase in the presence of PR H-8BN covalently coupled to PEG 6000 revealed a competitive type of inhibition with respect to FAD. The type of inhibition

Table 4
Comparison of the dissociation constants obtained from affinity partitioning and difference spectroscopy

Dye	Affinity partitioning		*n*	Difference spectroscopy
	K_{d_T} (μM)	K_{d_B} (μM)		K_d (μM)
Procion Red H-E3B	3.17	0.38	2	1.72
Procion Green H-E4BD	5.45	0.84	2	2.37
Procion Red H-3B	8.14	0.85	2	2.24
Procion Red MX-5B	50.34	4.48	2	12.48
Procion Red MX-8B	34.79	3.00	2	0.14
Procion Red H-8BN	3.29	0.44	2	2.72
Cibacron Blue F3G-A	27.70	2.95	2	1.60
Cibacron Blue 3G-A	55.72	19.58	2	5.59

NADH, $k_m = 3\ \mu M$; FAD, $K_m = 72\ \mu M$.

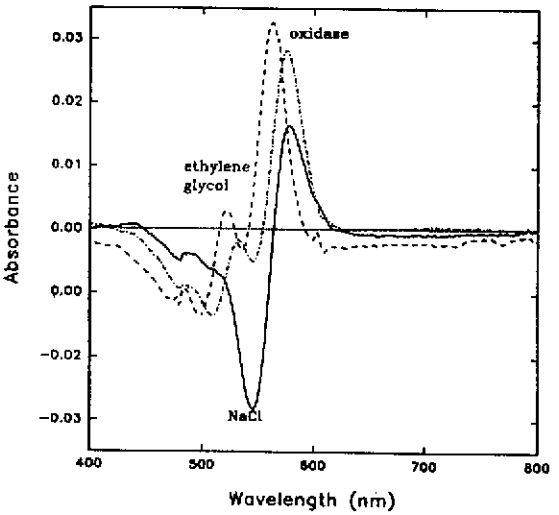

Fig. 4. Difference spectra of PR H-8BN. All spectra were recorded in 50 m*M* potassium phosphate buffer (pH 7.2) at 25°C in the presence of (——) 0.5 *M* NaCl at a dye concentration of 28.9 μM, (– – –) 50% (v/v) ethylene glycol at a dye concentration of 2.5 μM and (–·–·–) 0.9 μM NADH oxidase at a dye concentration of 2.7 μM.

Table 5
Influence of FAD and NADH on the affinity partitioning of NADH oxidase

Dye–PEG	Remaining Δ log K (%)[a]	
	2 m*M* FAD	4 m*M* NADH
Procion Red H-E3B	100	68
Procion Green H-E4BD	26	71
Procion Red H-3B	62	65
Procion Red MX-5B	100	52
Procion Red MX-8B	43	62
Procion Red H-8BN	48	74
Cibacron Blue F3G-A	59	71
Cibacron Blue 3G-A	67	73

The systems (2 g) contained 13.5% (w/w) dextran T10, 9% (w/w) PEG 6000, 50 m*M* potassium phosphate buffer (pH 7.2), 4 m*M* NADH or 2 m*M* FAD and 5 units of enzyme. The partitioning was performed at 25°C.
[a] Δ log K in the absence of NADH or FAD was taken as 100%.

with respect to NADH is not easy to distinguish. Both non- and uncompetitive effects are possible. The calculated kinetic constants are summarized in Table 7. All estimated inhibition constants (K_i; K_{ii}; K_{iii}) are significantly lower than the K_m for NADH and FAD, corroborating the finding of the high affinity of the dye ligand.

4. Discussion

This study has shown that affinity partitioning of NADH oxidase from *Thermus thermophilus* HB8 in aqueous two-phase systems is applicable to the study of the interaction of the enzyme with biomimetic dye ligands. The method seems to be sensitive enough to recognize even small differences in the affinity of the dye to the target enzyme which can be caused either by structural alterations of the dye ligand or by addition of competing effectors.

In comparison with difference spectroscopic studies applying the free dye and to kinetic analysis using dye-liganded PEG, the specific environment of a two-phase system [polymer concentrations up to 25% (w/w)] and the covalent attachment of the dye to PEG has to be taken into account. Therefore, dissociation constants obtained by difference spectroscopy, kinetics and affinity partitioning are not identical as free dyes bind with higher affinity than the polymer-coupled ligands and the affinity of the free dye ligand as well as the polymer-bound dye decreases with increasing concentration of PEG. This behaviour has been shown by inhibition studies with NADH oxidase and alkaline phosphatase from calf intestine in buffer–polymer mixtures (unpublished data) and from fluorescence spectroscopic measurements [17,18]. In conclusion, the study of dye–enzyme interaction using the free ligand cannot *per se* predict quantitatively the binding behaviour of the biomimetic dye in a conjugated form.

The present state of the knowledge about the chemistry of interaction of NADH oxidase from *Thermus thermophilus* HB8 and various triazine dyes can be summarized as follows:

(i) The binding of triazine dyes to NADH oxidase from *Thermus thermophilus* HB8 is realised by hydrophobic and electrostatic forces. This follows from the results of affinity chromatography (elution with ethylene glycol) and from the difference spectroscopic data. The low influence of ionic strength on affinity chromatography of the enzyme can be caused by the coupling of the dye to the matrix, which could decrease the accessibility of the negatively charged terminal ring of the dye ligand.

(ii) The binding of the dye ligands involves in most instances the FAD binding site of the enzyme. The extent to which the NADH-binding region is involved in the binding of the dye cannot be elucidated.

(iii) Small changes in the structure of the dye ligands can alter the binding properties drastically. PR H-E3B, which interacts with other flavoproteins [19,20], binds the NADH oxidase from *Thermus thermophilus* HB8 with high affinity but shows no change of interaction in the presence of FAD. PG H-E4BD seems to be a good biomimetic ligand for NADH oxidase, because a strong competition with FAD was found. Similarly, NADH oxidase from *Streptococcus faecalis* containing tightly bound FAD also possesses a high affinity to this dye ligand. However, the

Table 6
Influence of NADH and FAD on affinity chromatography and difference spectroscopy of NADH oxidase

Affinity chromatography							
Effector[a]	Dye-liganded Sepharose 4B						
	PR H-E3B	PG H-E4BD	PR H-3B	PR MX-5B	PR MX-8B	PR H-8BN	CB F3G-A
	Activity eluted (%)[b]						
NADH (4 m*M*)	0	3	0	19	3	27	28
FAD (2 m*M*)	0	52	14	0	25	35	26
NaCl (500 m*M*)	0	5	20	0	0	18	10
Ethylene glycol (50%, v/v)	0	95	99	92	95	99	92
Difference spectroscopy with free dyes							
Effector[a]	Quenching of the signal (%)[c]						
Effect of NADH (4 m*M*)	2	5	2	20	1	2	5
Effect of FAD (1 m*M*)	1	49	57	10	48	71	87
Type of interaction[d]	m	m	n.d.	m	m	m	m

All measurements were performed in 50 m*M* potassium phosphate buffer (pH 7.2) at 25°C.
[a] Dissolved in 50 m*M* potassium phosphate buffer (pH 7.2) at 25°C.
[b] Total bound activity was taken as 100%.
[c] Decrease of signal ($absorbance_{max} - absorbance_{min}$); the signal of the dye-saturated enzyme was taken as 100%.
[d] m = mixed; n.d. = not detectable.

Table 7
Inhibition of NADH oxidase by PR H-8BN covalently coupled to PEG 6000

Inhibition with respect to	Type of inhibition and kinetic constants (μM)					
	Competitive		Non-competitive		Uncompetitive	
	K_i	K_m	K_{ii}	K_m	K_{iii}	K_m
FAD (NADH constant at 173 μM)	0.07	72.2	–	–	–	–
NADH (FAD constant at 127 μM)	–	–	0.11	3.38	0.12	2.81

All measurements were made at 25°C in 50 m*M* potassium phosphate buffer (pH 7.2). Inhibition constants and K_m values were calculated at a constant concentration of NADH (173 μM) and varying the FAD concentration from 12 to 127 μM at dye–PEG concentrations between 0 and 0.12 μM and at a constant FAD concentration (127 μM) by varying the NADH concentration in the range 2–173 μM at dye–PEG concentrations between 0 and 0.25 μM, respectively.

dye–enzyme interaction can be diminished by both FAD and NADH [19]. CB F3G-A binds the NADH oxidase from *Thermus thermophilus* with only moderate affinity at its nucleotide binding site(s). However, the dye ligand has been successfully used in the affinity chromatography of this enzyme [1,12] and in the purification of other flavoproteins exhibiting tightly bound FAD [21–25].

(iv) The available data do not allow to predict all structural requirements of a dye acting as an optimum biomimetic ligand of NADH oxidase from *Thermus thermophilus* HB8. However, by summarizing all data, a structural model that fulfils basic requirements for binding can be proposed (Fig. 5).

The presence of a disulphonated aminonaphthol ring in combination with another aromatic negatively charged residue and a hydrophobic arm seems to be a good prerequisite to bind the enzyme with high affinity. A conformational analysis of the ligand structure by using molecular modelling (MOBY, Version 1.4; Springer, Berlin, Germany) gave distances between the negatively charged sulphonic acid group and the hydrophobic arm in the range 7–13 Å.

A comparison of all the dyes used revealed that the dye ligand PR H-8BN (for structure, see Fig. 3) fits best with the proposed model. It binds to the enzyme with high affinity and shows strong competition to the FAD binding site with an involvement of the NADH binding region.

As shown by X-ray diffraction analysis of the holoenzyme, there are two FAD binding sites per enzyme dimer with the fixation of the FAD molecules in the two clefts between both subunits stabilised by electrostatic forces between the phosphate group(s) of the cofactor and Arg_{17}, Arg_{21} and Arg_{195} and by hydrophobic interactions between Ala_{46} and Leu_{158} and the isoalloxazine ring of the flavin nucleotide [2]. A first preliminary X-ray diffraction analysis of an enzyme–PR H-8BN complex showed that the FAD cofactor is completely displaced by soaking the crystal with this dye ligand. The formation of the enzyme–dye complex seems to cause some smaller changes in the conformation in the FAD pocket, but the position of one phosphate group of the cofactor seems to be occupied by a sulphonic acid group of the dye with similar electrostatic interactions to arginine residues.

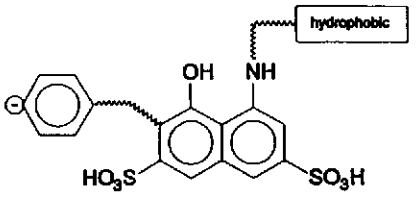

Fig. 5. Model for a biomimetic ligand of NADH oxidase from *Thermus thermophilus* HB8.

The preliminary crystallographic data are in accordance with the results of affinity partitioning, difference spectroscopy and kinetics, suggesting that PR H-8BN occupies both FAD binding sites of the enzyme.

5. References

[1] H.-J. Park, C.O. Reiser, S. Kondruweit, H. Erdmann, R.D. Schmid and M. Sprinzl, *Eur. J. Biochem.*, 205 (1992) 881.
[2] H.-J. Hecht, H. Erdmann, H.-J. Park, M. Sprinzl, R.D. Schmid and D. Schomburg, presented at the *16th Congress of the International Union of Crystallography, Beijing, China, August 21–29, 1993.*
[3] D. Pompon and F. Lederer, *Eur. J. Biochem.*, 90 (1978) 563.
[4] T. Prestera, H.J. Prochaska and P. Talalay, *Biochemistry*, 31 (1992) 824.
[5] Y.C. Tsai, T.Y. Yang, S.W. Cheng, S.N. Li and Y.J. Wang, *Prep. Biochem.*, 21 (1991) 175.
[6] C.R. Lowe, S.J. Burton, N.P. Burton, W.K. Alderton, J.M. Pitts and J.A. Thomas, *Trends Biotechnol.*, 10 (1992) 442.
[7] H. Erdmann, H.-J. Hecht, H.-J. Park, M. Sprinzl, D. Schomburg and R.D. Schmid, *J. Mol. Biol.*, 230 (1993) 1086.
[8] C.R. Lowe and J.C. Pearson, *Methods Enzymol.*, 104C (1984) 97.
[9] G. Johansson, *Methods Enzymol.*, 104C (1984) 356.
[10] J. Kirchberger, F. Cadelis, G. Kopperschläger and M.A. Vijayalakshmi, *J. Chromatogr.*, 483 (1989) 289.
[11] P. Hughes, C.R. Lowe and R.F. Sherwood, *Biochim. Biophys. Acta*, 700 (1982) 90.
[12] H. Erdmann, H.-J. Hecht and R.D. Schmid, *Dechema Biotechnol. Conf.*, 5 (1992) 93.

[13] W.H. Press, B.P. Flannery, S.A. Teukolsky and W.T. Vetterling, *Numerical Recipes, the Art of Scientific Computing*, Cambrdige University Press, Cambridge, 1988.
[14] S.D. Flanagan and S.H. Barondes, *J. Biol. Chem.*, 250 (1975) 1484.
[15] S. Subramaniam, *Arch. Biochem. Biophys.*, 216 (1982) 116.
[16] R.E. Barden, P.L. Darke, R.A. Deems and E.A. Dennis, *Biochemistry*, 19 (1980) 1621.
[17] A. Cordes, J. Flossdorf and M.R. Kula, *Biotechnol. Bioeng.*, 30 (1987) 514.
[18] P.A. Alred, G. Johansson and F. Tjerneld, *Anal. Biochem.*, 205 (1992) 351.
[19] H.-L. Schmidt, W. Stöcklein, J. Danzer, P. Kirch and B. Limbach, *Eur. J. Biochem.*, 156 (1986) 149.
[20] V. Radjendirane, M.A. Bhat and C.S. Vaidyanathan, *Arch. Biochem. Biophys.*, 288 (1991) 169.
[21] J. Leonil, S. Langrene, S. Sicsic and F. Le Goffic, *J. Chromatogr.*, 347 (1985) 316.
[22] H.J. Prochaska, *Arch. Biochem. Biophys.*, 267 (1988) 529.
[23] D.H. Sharkis and R.P. Swenson, *Biochem. Biophys. Res. Commun.*, 161 (1989) 434.
[24] Q. Ma, R. Wang, C.S. Yang and A.Y. Lu, *Arch. Biochem. Biophys.*, 283 (1990) 311.
[25] C.M. Yea, A.R. Cross and O.T. Jones, *Biochem. J.*, 265 (1990) 95.